*NASA/CR-97-*

*JNAS 5-2706*

*IN-93-CR*

*(E)Carived*

*067294*

**207141**

# X-RAY EMISSION FROM THE GUITAR NEBULA

ROGER W. ROMANI[1]

Department of Physics, Stanford University, Stanford, CA 94305-4060

JAMES M. CORDES[2]

Astronomy Department and NAIC, Cornell University, Ithaca, NY 14853

AND

I.-A. YADIGAROGLU

Department of Physics, Stanford University, Stanford, CA 94305-4060

*Received 1996 October 28; accepted 1997 May 19*

## ABSTRACT

We have detected weak soft X-ray emission from the pulsar wind nebula trailing the high-velocity star PSR 2224+65 (the "Guitar Nebula"). This X-ray flux gives evidence of $\gamma \sim 10^7$ eV particles in the pulsar wind and constrains the properties of the postshock flow. The X-ray emission is most easily understood if the shocked pulsar wind is partly confined in the nebula and if magnetic fields in this zone can grow to near-equipartition values.

*Subject headings:* ISM: jets and outflows — pulsars: individual (PSR 2224+65) — X-rays: ISM

## I. INTRODUCTION

Identifying the spin-down products of rotation-powered pulsars is a long-standing problem in astrophysics. Recent observations of high-energy emission from young pulsars (e.g., Fierro 1996) and improvement in emission models (e.g., Romani 1996) show that up to a few $\times 10\%$ of the spin-down power can be ascribed to observed photons. In most cases, the remaining power in particles and unobserved radiation still need to be identified. The wind of energetic particles and fields emitted from spin-powered pulsars is most easily observed when it is confined. Such postshock, or "plerionic," emission has long been associated with sources such as the Crab and Vela pulsars and with similar filled-center remnants such as 3C 58, presumably containing young pulsars.

The discovery of bow shock nebulae around a number of pulsars has provided a further opportunity to study pulsar winds. These nebulae generally occur when the pulsar is either long lived, with a low magnetic field B and a short spin period, or when it has a large space velocity; these properties allow escape from the parent supernova remnant of the pulsar while it retains substantial spin-down power. The pulsar wind then shocks against the ambient interstellar medium (ISM). These objects are most prominent as $H\alpha$ nebulae, first discovered around the millisecond pulsar PSR 1957+20 (Kulkarni & Hester 1988; see also Aldcroft, Romani, & Cordes 1992). A similar bow shock is seen around the 5 ms pulsar PSR J0437−4715 (Bell, Bailes, & Bessel 1993), and Cordes, Romani, & Lundgren (1993, hereafter CRL) have detected an $H\alpha$ nebula around the high-velocity, slow-spin pulsar PSR 2224+65.

High-energy observations of these pulsar wind nebulae (PWNs) can place key constraints on the pulsar particle output. Models of the Crab Nebula (Kennel & Coroniti 1984), for example, indicate that the bulk of the spin-down power is carried off in an $e^\pm$ wind with $\gamma \sim 10^{6.5}$. Arons & Tavani (1993) described the expected high-energy emission from wind shocks

[1] Alfred P. Sloan Fellow; rwr@astro.stanford.edu.

[2] cordes@astrosun.tn.cornell.edu.

in the PSR 1957+20 system, focusing on a wind model including a massive baryonic component. Using the *ROSAT* Position Sensitive Proportional Counter (PSPC) observations of PSR 1957+20, Kulkarni et al. (1992) were able to extract general constraints on the $e^\pm$ content of the pulsar wind. A trail of soft X-ray emission behind the nearby pulsar PSR 1929+10, discovered in *ROSAT* PSPC data by D. Helfand and described by Wang, Li, & Begelman (1993), is also a likely product of pulsar wind-ISM interaction. Finally, the interaction of pulsar winds with companion stellar winds can also produce a bow shock geometry. For example, PSR 1259−63 in an eccentric orbit around a Be companion provides the opportunity of studying the pulsar wind interactions under changing conditions (Arons & Tavani 1994). *ASCA* observations of nonthermal X-rays (see Hirayama 1996, and references therein) have in particular provided important constraints on the particle energy and luminosity.

We describe here *ROSAT* High-Resolution Imager (HRI) observations of the PWN trailing PSR 2224+65, the "Guitar Nebula." This is followed by a description of the bow shock flow geometry and a discussion of the origin of the observed X-ray flux. The Guitar Nebula is particularly interesting because the pulsar itself is relatively normal, but the high velocity and peculiar shock geometry of the system provide opportunities to probe the pulsar wind interactions under conditions quite different than those found in other PWNs. In particular, the small bow shock scale allows soft X-ray constraints on electron energies similar to those inferred for the Crab pulsar.

## 2. *ROSAT* HRI FLUX

We proposed *ROSAT* HRI observations of PSR 2224+65 to detect emission in the shocked wind and ISM and to constrain the physics of the postshock flow. Exposures were obtained in seven observation intervals during 1994 July 13–25. With 36,894 s of dead-time corrected exposure centered on PSR 2224+65 we were able to detect coronal emission from about 10 bright stars in the field. Cross-correlation with optical
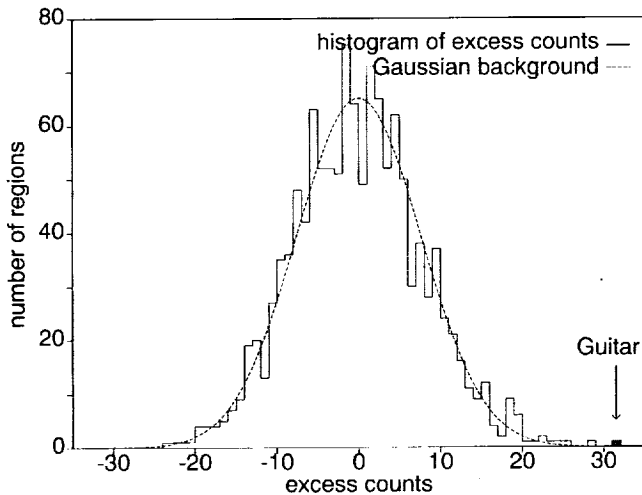
Fıg. 2.—Histogram of excess counts in nonoverlapping guitar-shaped apertures in the HRI image. The observed counts at the Guitar Nebula position are in the shaded bin.

frames registered to deep Hα images showing the Guitar Nebula allowed us to "bore-sight" the HRI data. Three *Hubble Space Telescope* (*HST*) guide stars (GSC 472−144, −188, −232) were detected with standard processing in the center of the HRI frame and were used for final alignment of the X-ray and optical images to less than 1″. This allowed a very sensitive search for emission from PSR 2224+65 and the Guitar Nebula. No X-ray emission was detected from PSR 2224+65 itself, with the 2 counts detected within 4″ of the pulsar position entirely consistent with the 2.02 counts expected from the mean background rate. However, an X-ray excess was apparent in the vicinity of the Hα nebula. We have defined an aperture of half-width 4″ following the outline of the edge-brightened guitar shape. If the X-ray emission is confined to the limb, then this contour will contain 90% of the source counts; if the bubble interior has X-ray emission, then the omitted flux will be slightly larger. This contour contains 31 counts at the Guitar Nebula position in excess of the 58 counts expected from the mean background rate (Fig. 1 [Pl. L19]). This is formally a 4.1 σ detection. To check the significance, we summed counts in our nebula-shaped aperture at various independent positions in the HRI image, after applying vignetting corrections and excluding regions where significant point sources (generally identified stars) were found in the standard PROS processing. The histogram of the resulting excess counts (Fig. 2) shows that the true Guitar Nebula position has the largest excess. Estimating the envelope of the count fluctuations again gives a significance slightly in excess of 4 σ. The Guitar Nebula thus emits soft X-rays with a count rate of $9.6 \times 10^{-4}$ counts s$^{-1}$ in the *ROSAT* band. The flux seems to follow the limb of the Guitar Nebula, concentrating in the forward facing parts of the nebula, but starting significantly behind the pulsar itself.

Some crude spectral information is available from the PHA energy channels in the HRI detector. We find that the excess Guitar Nebula counts are soft, with a median PHA channel of 6. The distribution is only slightly harder than that of the mean background counts, but it also contains an excess of counts in PHA channels 0–1, suggesting UV flux near the source. This "spectrum" is clearly different from some of the stronger sources identified with bright stars in the optical; these have

median PHA channels of 8–9 and very few counts below channel 5. Unfortunately, with the very low count rate and lack of calibration, quantitative results cannot be extracted from this hardness information.

The implied X-ray luminosity is sensitive to the parent spectrum and the absorption. From the pulsar dispersion measure (DM) 35.3 cm$^{-3}$ pc$^{-1}$ and an assumed $n_e/n_H = 0.1$ we infer a column density $N_H \approx 10^{21}$ cm$^{-2}$. This assumed $n_e/n_H$ is very similar to that inferred for PSR 2334+61 (Becker, Brazier, & Trümper 1996) at a similar direction and DM. The Balmer decrement in the Guitar Nebula itself suggests $A_V = 1.65$, corresponding to $N_H = 3 \times 10^{21}$ cm$^{-2}$. However, because the Balmer ratios in nonradiative shocks are uncertain (Chevalier, Kirshner, & Raymond 1980; Raymond 1991), we adopt here $10^{21}$ for the absorbing column. With this $N_H$ and a photon number index of $\alpha = 2$, we infer an X-ray flux of $1.8 \times 10^{-13}$ ergs cm$^{-2}$ s$^{-1}$ (0.01–10 keV); for $N_H = 3 \times 10^{21}$ cm$^{-2}$ the flux is 50% higher. This represents $1.7 \times 10^{-2} d_{\rm kpc}^2 / I_{45}$ of the spin-down luminosity.

## 3. GEOMETRY OF THE GUITAR NEBULA

As described in CRL, the Guitar Nebula is an Hα-emitting bow shock trailing the slow-spin ($P = 0.68$ s), intermediate-age ($\tau_c = 1.1 \times 10^6$ yr) pulsar PSR 2224+65. With an interferometrically determined proper motion giving a space velocity of $v_p = 8.4 \times 10^7 d_{\rm kpc}/\cos i$ cm s$^{-1}$ (with $i$ being the angle between the velocity and the plane of the sky) and a DM distance estimate of $d_{\rm kpc} = 1.95$ kpc (Taylor & Cordes 1993), this object has arguably the highest space velocity of any known star.

With this velocity the standoff of the pulsar wind bow shock is especially small for this nebula. The pulsar spin-down luminosity $\dot{E} = 1.3 \times 10^{33} I_{45}$ ergs s$^{-1}$ is believed to power a relativistic wind that shocks against the ISM of density $\rho = 2.2 \times 10^{-24} n_H$ g cm$^{-3}$, giving a momentum balance standoff of the contact discontinuity at the bow shock nose of

$$r_0 = \left(\frac{\dot{E}}{4\pi c \rho v_p^2}\right)^{1/2} = 4.7 \times 10^{14} \left(\frac{I_{45}}{n_H}\right)^{1/2} \cos i / d_{\rm kpc} \ {\rm cm}. \quad (1)$$

The Balmer emission of PWNs is caused by neutral ISM atoms drifting into the shocked gas and suffering collisional excitation or charge exchange into excited states of the post-shock ions. Accordingly, Hα arises in a thin sheet behind the ISM shock, upstream from the contact discontinuity (Chevalier, Kirshner, & Raymond 1980). A detailed model for the bow shock flow is not available, but Aldcroft et al. (1992) estimated that the Hα apex lies at about $1.3r_0$. This size was unresolved in ground-based images of the Guitar Nebula. *HST* Wide Field Planetary Camera (WFPC2) Hα images of the nebula, however, show that the apex has the classic bow shock shape displayed by the PSR 1957+32 and PSR J0437−4715 nebulae. These data are described elsewhere (Cordes et al. 1997). Here we note only that while the pulsar, and hence the standoff angle, are not directly observed in the *HST* data, a fit to the bright Hα ridge of the bow shock allows us to measure the size of the bow shock and infer $r_0$. Wilkin (1996) has derived convenient analytic expressions for the geometry of a thin momentum-balance bow shock. Assuming that the shock standoff at the apex scales proportionally for the rest of the bow wave, the scaled version of the momentum-balance contact discontinuity curve gives the following bow shock shape:

$$\theta_{\rm H\alpha}(\phi) = 1.3r(\phi)/d = 1.3r_0 \csc \phi \sqrt{3(1 - \phi \cot \phi)}/d, \quad (2)$$

where the pulsar is at the origin and position angle $\phi$ is measured from the pulsar velocity. The fit determines the origin and the overall scale, giving an inferred H$\alpha$ standoff angle as $\theta_{H\alpha}(0) = 0\rlap{.}''038 \pm 0\rlap{.}''005$. This corresponds to a contact discontinuity scale $r_0 = 4.3 \times 10^{14}d_{kpc}/\cos i$ cm, which with equation (1) gives an estimate of the pulsar distance as $d_{kpc} = 1.1 \cos i \ (I_{45}/n_{11})^{1/4}$.

Ground-based Palomar 200" images (Fig. 1) show that the shape of the H$\alpha$ nebula downstream from the *HST* resolved apex can be described as an approximately $3'' \times 20''$ tube (the "neck" of the guitar) connecting to a complex bubble that flares gradually to a diameter of about 30" some 70" behind the pulsar. The waist in this bubble (the guitar "body") may be due to ISM density variations. The bubble also does not appear fully closed at the end opposite the pulsar. With the observed proper motion, the pulsar traverses the Guitar Nebula in about 430 yr. CRL give the H$\alpha$ flux of the head of the nebula as $1.1 \times 10^{-3}$ photons cm$^{-2}$ s$^{-1}$. This line flux implies that neutral H atoms enter the nebula head at $1.3 \times 10^{41}d_{kpc}^2$ atoms s$^{-1}$. With the observed radius of about $1\rlap{.}''5$, an ISM neutral fraction $X$, and the measured pulsar proper motion, the nebula head should sweep up neutral H at $1.3 \times 10^{41}n_Hd_{kpc}^3/X$ atoms s$^{-1}$. Thus, the observed line flux is in good accord with the *HST* constraints on the bow shock geometry for $n_Hd_{kpc}/X \sim 1$.

The variation in nebula cross section can be understood from pressure balance arguments. Behind the pulsar the outflowing wind drives the bow shock tail into the ISM; this stalls where the wind ram pressure balances the ISM static pressure $(10^{-12} P_{-12}$ g cm$^{-1}$ s$^{-2})$. Well behind the pulsar the wind impacts at a shallow angle; a characteristic position angle of $\phi \sim 150°$ gives a transverse pressure of approximately $\dot{E}$ $\sin^3(\pi - \phi)/(4\pi\theta_\perp^2 d^2 c) \sim 2 \times 10^{-12}I_{45}(\theta_\perp'' d_{kpc})^{-2}$ g cm$^{-1}$ s$^{-2}$ in a tube of radius $\theta_\perp''$. Thus, we expect the ram pressure–driven "neck" of the Guitar Nebula to stall at a width $\theta_\perp \sim 1\rlap{.}''4(I_{45}/P_{-12})^{1/2}/d_{kpc}$. Farther downstream it is clear that the shocked pulsar wind is partly confined in the body of the Guitar Nebula. This confinement may be aided by the increased ram pressure associated with expansion into a dense region toward the rear of the Guitar Nebula, delimited by the horizontal filament in Figure 1. Here the isotropic pressure of the shocked relativistic plasma $P_{rel} = u/3$ comes into play. If the wind emitted during the time the pulsar crosses the Guitar Nebula is fully confined in a tube of diameter $r_\perp$ and there is no cooling, then the pressure is $\dot{E}/(3\pi r_\perp^2 v_p)$. In practice, the back of the nebula does not appear closed, so perhaps about 0.1 of this pressure obtains; even with this pressure the bubble stalls with a characteristic radius $\theta_\perp \approx 26''(I_{45}/P_{-12})^{1/2}d_{kpc}^{3/2}$. We thus have a consistent picture of the Guitar Nebula bubble as a classic bow shock whose ram pressure stalls against the static ISM pressure behind the pulsar; the backflow in this neck should be mildly relativistic. Further downstream, the shocked pulsar wind stalls and becomes partly confined. The shocked wind expands against the ISM, inflating the bubble to the observed approximately 30" diameter.

### 4. IMPLICATIONS AND BOW SHOCK FLOW

We turn now to the interpretation of the lack of X-ray flux from PSR 2224+65 and to the X-ray flux from the Guitar Nebula body. The nondetection of the pulsar is not surprising. At $\tau_c = 10^6$ yr the expected surface temperature of approximately $3 \times 10^5$ K from standard cooling models predicts a

luminosity of approximately $6 \times 10^{30}$ ergs s$^{-1}$ and no significant HRI flux. Pulsars of similar age have been detected by *ROSAT*, e.g., PSR 1929+10 (Yancopoulos, Hamilton, & Helfand 1994) and PSR 0823+26 (Sun et al. 1993), but the emission from these nearby objects seems to be from a small heated polar cap; scaled to the distance of PSR 2224+65 the polar cap flux of PSR 1929+10 would contribute less than 1 count in our exposure.

The two plausible sources of the nebular X-ray emission are the shocked pulsar wind and the postshock ISM. In contrast to the bow shocks around the slower pulsars PSR 1957+20 and PSR J0437$-$4715, the large pulsar velocity here gives high $T$ values in the shocked ISM gas; at the apex of the bow wave, the postshock ISM temperature is $3 \times 10^7d_{kpc}^2$ K. However, the small working surface resulting from the small $r_0$ value means that the shock luminosity near the guitar nose is only $\sim \pi r_0^2\rho v_p^3/$ $(2-8) \times 10^{29} n_{11}^{1/2}d_{kpc}^2$ ergs s$^{-1}$. Moreover, for a typical ISM abundance and cooling rate $\Lambda$, the characteristic cooling time $3kT/(8n_H\Lambda) \sim 8 \times 10^{13}n_{11}^{-1}$ s is quite long, so little thermal emission is expected before adiabatic losses in the postshock flow become significant. The absence of efficient cooling is supported by the Balmer-dominated nebular spectrum at the apex (CRL), which indicates that the shock is nonradiative (Chevalier et al. 1980). Along the body of the guitar, the continued expansion of the partly confined pulsar wind drives shock waves into the surrounding medium at $\bar{v} \sim 1.5 \times 10^7d_{kpc}$ cm s$^{-1}$. The implied shock luminosity along the guitar body is $L_{sh} \sim 2 \times 10^{32}d_{kpc}^3 n_{11}$ ergs s$^{-1}$, with a postshock temperature of about $4 \times 10^5d_{kpc}^2$ K. Although the cooling time for $d_{kpc} \sim 1$ is comparable to the flow time through the nebula (so that we might expect some thermal emission from the tail of the guitar), the effective temperature is too low to produce the observed HRI count rate. Even if the distance to PSR 2224+65 is as large as 2 kpc, prospects for thermal emission from the nebula are not much better. With $T_{sh} = 1.6 \times 10^6$ K our observed HRI counts imply a thermal luminosity at 2 kpc of $8 \times 10^{32}$ ergs s$^{-1}$ for $N_H = 10^{21}$ cm$^{-2}$ and a Raymond-Smith thermal spectrum. However, at these temperatures the cooling time is about $3 \times 10^{12}n_{11}^{-1}$ s, so that radiation in the postshock flow is inefficient. Thus, unless $d_{kpc}$ and $n_{11}$ are large, $N_H$ is small, and the cooling rate is significantly enhanced, thermal emission cannot account for the observed HRI flux.

A more promising source is postshock synchrotron cooling of the relativistic pulsar wind. In the ram pressure balance region of the bow wave, the energy dissipated in this shocked wind is larger than that in the shocked ISM by $c/v_p \sim 300$. Observations of the Crab nebula plerion suggest that the pulsar wind is dominated by energetic $e^\pm$ with $\gamma = 10^7\gamma_7$, $\gamma_7 \sim 0.3$. These electrons radiate in the postshock field of the pulsar wind, $B_s = 2 \times 10^{-3}(r_0/r)$. Kulkarni et al. (1992) were able to use the X-ray flux from the millisecond pulsar PSR 1957+20 to limit the fraction of the pulsar spin-down in $e^\pm$ with $\gamma_7 \sim 0.01$ and $\gamma_7 \sim 10$, assuming synchrotron emission at the companion shock and at the bow shock, respectively. With its larger field and high velocity, the soft X-ray flux of PSR 2224+65 is most sensitive to intermediate electron energies, similar to those in the Crab Nebula. Including the $r^{-1}$ dependence of the pulsar wind $B$ we find that the synchrotron spectrum in the shocked wind has a peak energy $E_c \approx 3.5(r_0/r)\gamma_7^2$ keV, so that closer than $r_{max} \sim 15\gamma_7^2r_0$ the charges will radiate in the *ROSAT* band.

We expect the shocked pulsar wind to have a mildly relativistic backflow in the bow shock, with a characteristic

flow time at a distance $r$ from the pulsar of $\tau_{fl} \sim 3r/c$. This is shorter than the synchrotron cooling time under these conditions, so that the efficiency is small, $\eta \sim \tau_{fl}/\tau_{sy} \sim 3 \times 10^{-3}(r_0/r)\gamma_7$. When the peak energy is well above the ROSAT threshold the observed flux will decrease somewhat; since the synchrotron emissivity at energy $E$ scales approximately as $E^{1/3}$ exp $(-E/E_c)$, the fraction of the radiation in the ROSAT band has the weak dependence $(0.3 \text{ keV}/E_c)^{1/3} \sim 0.4(r/r_0)^{1/3}\gamma_7^{2/3}$. Thus, if a fraction $f_\gamma$ of the spin-down energy is carried off by charges of Lorentz factor $\gamma$, then including the cooling efficiency and the fraction of the spectrum in the ROSAT band, we get an observed X-ray luminosity from the wind shock within position angle $\phi$ of

$$L_x \sim 10^{-3} f_\gamma \dot{E}(1 - \cos \phi) \left[\frac{r_0}{r(\phi)}\right]^{2/3} \gamma_7^{1/3},$$

where $r(\phi)$ is determined from equation (2). Thus, the emission should be concentrated toward the bow shock apex. Because the wind cannot cool effectively before the relativistic backflow carries it toward the body of the guitar, the total luminosity is small. With an $\alpha = 2$ spectrum and $N_H = 10^{21}$ cm$^{-2}$ at 1 kpc, we expect 2 counts from the shocked pulsar wind at the apex of the flow.

Above we have assumed that the field in the pulsar wind itself dominates $B$ in the postshock region and that the flow is not confined. However, it appears that the pulsar wind is partly confined in the nebula. In addition, turbulence in the shocked pulsar wind may increase $B$ up to equipartition values. At the shock apex $B_{eq} \ll B_s$, so that our previous estimates hold. However, about $30r_0$ ($\sim 1''$) behind the pulsar the ram pressure associated with the sideways expansion of the guitar body at $1.5 \times 10^7 d_{kpc}$ cm s$^{-1}$ begins to exceed $B^2/4\pi$ in the shocked pulsar wind. Thus, as the neck of the Guitar Nebula merges into the body we expect that an equipartition field can reach $B_{eq} \sim 8 \times 10^{-5} d_{kpc} n_H^{1/2}$ G. The characteristic energy in this field $E_c \sim 0.15\gamma_7^2$ keV is large enough to contribute significant ROSAT emission. More importantly, if the shocked wind is partly confined in this region, we expect $\tau_{fl} \sim r/v_p \sim 5 \times 10^9$ s. For $d_{kpc} = 1$ we get a synchrotron cooling time $\tau_{sy} \sim 9 \times 10^9 \gamma_7^{-1}$ s and about 30% of the shock energy radiated in the ROSAT band for $\gamma_7 = 1$. This gives an observed X-ray flux $0.3\dot{E}f_\gamma\tau_{fl}/\tau_{sy}$. Thus, to produce the observed X-rays, we require $f_\gamma \sim 0.1$ in $\gamma_7 > 1$ particles. With the increased $B_{eq}$ inferred at 2 kpc, cooling is even more efficient, and we again infer $f_\gamma \approx 0.1$.

## 5. CONCLUSIONS

The X-ray emission observed from the bow shock created by PSR 2224+65 represents approximately $0.02d_{kpc}^2/L_{45}$ of its spin-down power. Although the large velocity of the pulsar ensures that gas is heated to X-ray emitting temperatures near the bow wave, the cooling in the postshock ISM flow is inefficient. Little of the observed flux can be contributed by the shocked ISM. The location of the X-ray emission significantly downstream from the pulsars suggests that the most likely source of the flux is the shocked pulsar wind. However, to account for the observed flux we require this wind to be partly confined in the Guitar Nebula body and that turbulence in the shocked wind flow can amplify the magnetic field to near-equipartition vales. If these conditions apply, then the observed flux implies that more than 0.1 of the pulsar spin-down power is being emitted in $e^+$ with $\gamma \sim 10^7$. Our data then support the idea that a pair plasma with $\gamma \sim 10^6$–$10^7$ is a dominant component of the pulsar wind for normal nonrecycled pulsars. Such a wind is in reasonable accord with models of pulsar magnetosphere acceleration, but the pairs may also be accelerated in the postshock region itself. In contrast, the conditions inferred for the soft X-ray emission from the shock of PSR 1929+10 by Wang et al. (1993) suggest that $\gamma > 10^8$ pairs are responsible for the PSPC photons; it is perhaps significant that the flux from these pairs represents only $10^{-4}$ of the spin-down luminosity of PSR 1929+10.

A more complete description of thermal and nonthermal emission in the Guitar Nebula will require detailed hydrodynamic models of the backflow in the postshock region. For example, Raga, Cabrit, & Canuto (1995) find that there is mixing of the shocked fluids in a bow shock flow. While the presence of the relativistic pulsar wind means that their sums are not directly applicable to PSR 2224+65, such mixing could affect the estimates of cooling time in the postshock flow. Such modeling coupled with future high throughput X-ray observations could give important constraints on the pulsar wind in this unique system.

REFERENCES

Aldcroft, T. L., Romani, R. W., & Cordes, J. M. 1992, ApJ, 400, 638
Arons, J., & Tavani, M. 1993, ApJ, 403, 249
———. 1994, ApJS, 90, 797
Becker, W., Brazier, K. T. S., & Trümper, J. 1996, A&A, 306, 464
Bell, J. F., Bailes, M., & Bessel, M. S. 1993, Nature, 364, 603
Chevalier, R. A., Kirshner, R. P., & Raymond, J. C. 1980, ApJ, 235, 186
Cordes, J. M., Romani, R. W., & Lundgren, S. C. 1993, Nature, 362, 133
Cordes, J. M., et al. 1997, in preparation
Fierro, J. F. 1995, Ph.D. thesis, Stanford Univ.
Hirayama, M. 1996, Ph.D. thesis, Inst. Space & Astron. Sci.
Kennel, C. F., & Coroniti, F. C. 1984, ApJ, 283, 694
Kulkarni, S. R., & Hester, J. J. 1988, Nature, 335, 801
Kulkarni, S. R., Phinney, E. S., Evans, C. R., & Hasinger, G. R. 1992, Nature, 359, 300
Raga, A. C., Cabrit, S., & Canuto, J. 1995, MNRAS, 273, 422
Raymond, J. C. 1991, PASP, 103, 781
Romani, R. W. 1996, ApJ, 470, 469
Sun, X., Trümper, J., Dennerl, K., & Becker, W. 1993, IAU Circ., 5895
Taylor, J. H., & Cordes, J. M. 1993, ApJ, 411, 674
Wang, Q. D., Li, Z.-Y., & Begelman, M. C. 1993, Nature, 364, 127
Wilkin, F. P. 1996, ApJ, 459, L31
Yancopoulis, S., Hamilton, T. T., & Helfand, D. J. 1994, ApJ, 429, 832

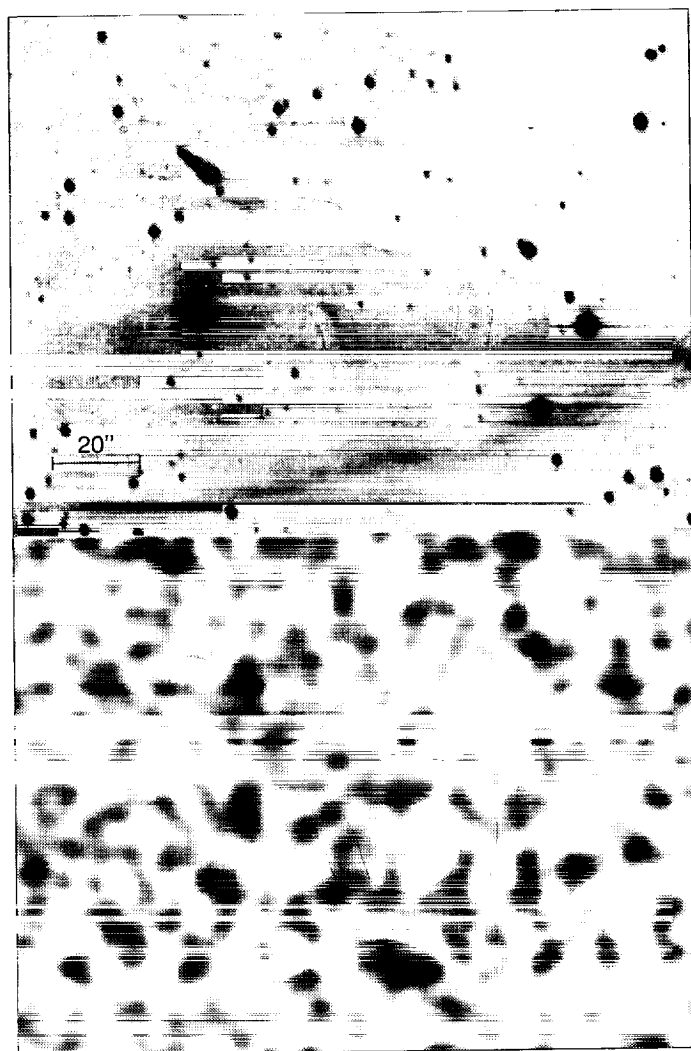FIG. 1.—*Top*: Hα image of the Guitar Nebula, showing our shaped aperture. *Bottom*: Aperture over central portion of the smoothed HRI count map.

ROMANI, CORDES, & YADIGAROGLU (see 484, L138)